J Mol Model (2013) 19:3733–3740
DOI 10.1007/s00894-013-1898-5

ORIGINAL PAPER

DFT studies of acrolein molecule adsorption on pristine and Al- doped graphenes

Somayeh F. Rastegar · Nasser L. Hadipour · Mohammad Bigdeli Tabar · Hamed Soleymanabadi

Received: 20 March 2013 / Accepted: 26 May 2013 / Published online: 22 June 2013

Abstract The ability of pristine graphene (PG) and Al-doped graphene (AlG) to detect toxic acrolein (C_3H_4O) was investigated by using density functional calculations. It was found that C_3H_4O molecule can be adsorbed on the PG and AlG with adsorption energies about −50.43 and – v30.92 kcal mol^{-1} corresponding to the most stable configurations, respectively. Despite the fact that interaction of C_3H_4O has no obvious effects on the of electronic properties of PG, the interaction between C_3H_4O and AlG can induce significant changes in the HOMO/LUMO energy gap of the sheet, altering its electrical conductivity which is beneficial to sensor designing. Thus, the AlG may be sensitive in the presence of C_3H_4O molecule and might be used in its sensor devices. Also, applying an external electric filed in an appropriate orientation (almost stronger than 0.01 a.u.) can energetically facilitate the adsorption of C_3H_4O molecule on the AlG.

Keywords Acrolein · Al-Doped graphene · DFT · Graphene · Sensor

Introduction

A material in the atmosphere which can cause harm to humans and the environment is known as an air pollutant. Pollutants can be in the form of solid particles, liquid droplets, or gases. As a liquid one, acrolein (C_3H_4O), is the simplest unsaturated aldehyde which is classified as a hazardous chemical because of its reactivity and flammability [1]. It is generated as a product of the incomplete combustion during forest and house fires, combustion of plastics, cooking food and mobile source emissions. A major source of C_3H_4O is cigarette smoke, which generates 50–90 ppm of C_3H_4O per cigarette. Some of the health risks associated with C_3H_4O are mutagenic and genotoxic to human cells [2]. It has been found to be both an acute and a chronic lung irritant [3]. So, determination of C_3H_4O concentration in the atmosphere, to keep the human's health and environmental safety, seems to be an important research. To approach this aim, methods with high detection limit are required. Sensors can help us to approaching to this goal.

An excellent gas sensor should have high sensitivity to the desired toxic material, as well as low cost production and a wide range of application [4]. Solid state sensors are well-known and widely used material for detection of toxic gases in the environment because of their exceptional sensitivity [5]. Today, solid-state sensors are available for detection of more than 150 different gases, including sensors for the gases which could otherwise only be detected using expensive analytical instruments.

In recent years, exploring some new-generation of nanomaterials opens quite new insight on the properties of this family with many potential application ranging from electronics [6, 7] to chemical sensors [8, 9]. Before Geim's group observed the single atomic layer of graphene in 2004 [10], having a finite sheet of thin carbons with just one atom thickness seemed a totally inaccessible dream. Graphene is an allotrope of carbon, composed by single-atomic layer of sp^2-bond carbon atoms which are closely and strongly packed in honeycomb crystal structure. It is a 2D building material that can be wrapped to 0D buckminsterfullerene, rolled into 1D carbon nanotube and stacked to 3D graphite. It has been noted that graphene can be a good candidate to detect various molecules, ranging from gas phase molecules

S. F. Rastegar · N. L. Hadipour (✉)
Department of Chemistry, Tarbiat Modares University, P.O. Box 14115-175, Tehran, Iran
e-mail: nasser.hadipour@yahoo.com

M. B. Tabar
Physics group, Science department, Islamic Azad University, Islamshahr Branch, P.O. Box: 33135-369, Islamshahr, Tehran, Iran

H. Soleymanabadi
Central Tehran Branch, Islamic Azad University, Tehran, Iran

to some small bioactive molecules [11]. The simplest graphene-based sensor reveals the conductivity change upon adsorption of molecules due to the changes of charge carrier concentration in the graphene. Since the first reported graphene-based gas sensor toward NO_2, NH_3, H_2O and CO by Shedin et al. in 2007 [12], there have been a number of theoretical [13, 14] and experimental [12, 15, 16] studies that investigated the gas sensing properties of mechanically exfoliated, chemically derived graphene and graphene oxide layers. Recently, we have shown that the Al-doped graphene (AlG) can be a good sensor for HCN [17].

While the sensitivity of pristine graphene (PG) and its derivatives toward some toxic molecules are widely examined [4, 12, 16, 18] to our knowledge, there is almost no investigation for C_3H_4O adsorption on PG and doped graphenes. So, the lack of such studies is felt. Therefore, it would be important to investigate whether the adsorption of C_3H_4O on PG and doped graphenes can be strong enough to introduce them as reasonable C_3H_4O sensors. The mentioned deficiency has motivated us to investigate the interaction of C_3H_4O with PG and AlG.

In this study, we investigated the sensitivity of both PG and AlG toward adsorption of toxic C_3H_4O. We considered some possible orientations of the C_3H_4O with respect to the adsorbents. The adsorption energies (E_a), the density of state (DOS) analyses, the structural parameters and the net electron transfers were calculated. Based upon the results, it was found that the electronic properties of AlG, contrary to what occurs in PG, are strongly altered in the presence of C_3H_4O. Desorption behavior of adsorbed C_3H_4O on AlG by applying an external electric field was also considered in this study.

Computational methods

All calculations were performed by GAMESS-US package [19] by using X3LYP functional with 6-31G(d) basis set. The X3LYP level of theory is an extended functional which significantly improves the accuracy for van der Waals interactions with respect to commonly used B3LYP functional [20]. A monolayer of PG was created and allowed to relax to its minimum energy structure (Fig. 1a). It contains 122 atoms (100 carbon and 22 hydrogen atoms) with zigzag edges. The edges were saturated with hydrogen atoms to neutralize the valances of terminal carbons, reducing edge effects. After relaxation, all C-C-C angles were calculated to be about 120° and, all the C-C and the C-H bond lengths about 1.425 and 1.086 Å, respectively which are in good agreement with reported values [21]. Tachikawa et al. [22] calculated values for the C–C and C–H bonds are about 1.420 and 1.088 Å, respectively, which have been obtained at B3LYP level of theory with 6-31G(d) basis set for a $C_{54}H_{18}$ graphene. Although infinite graphene sheets are intrinsically metallic (no distinct HOMO/LUMO energy gap (E_g) is expected), our PG system exhibits a semiconductor-like E_g (about 0.32 eV) due to size confinement. Shemella et al. [23] have been computationally shown that finite-sized graphene sheets have an E_g up to about 0.62 eV which will be decreased by increasing the size of the sheet.

The E_a of C_3H_4O molecule on the PG and AlG was calculated by using the following equation:

$$E_a = E_{C_3H_4O+adsorbent} - (E_{adsorbent} + E_{C_3H_4O}) + E_{BSSE} \quad (1)$$

where $E_{C3H4O+adsorbent}$, $E_{adsorbent}$, E_{C3H4O} are the energy of PG (or AlG) with absorbed C_3H_4O, the energy of isolated PG or AlG and the energy of the free C_3H_4O molecule, respectively. Basis set superposition error (BSSE) was computed to correct E_a, removing basis functions overlap effects. The charge transfer between the molecule and the surfaces was calculated by Mulliken charge analysis from the difference of the charge concentration on C_3H_4O before and after adsorption.

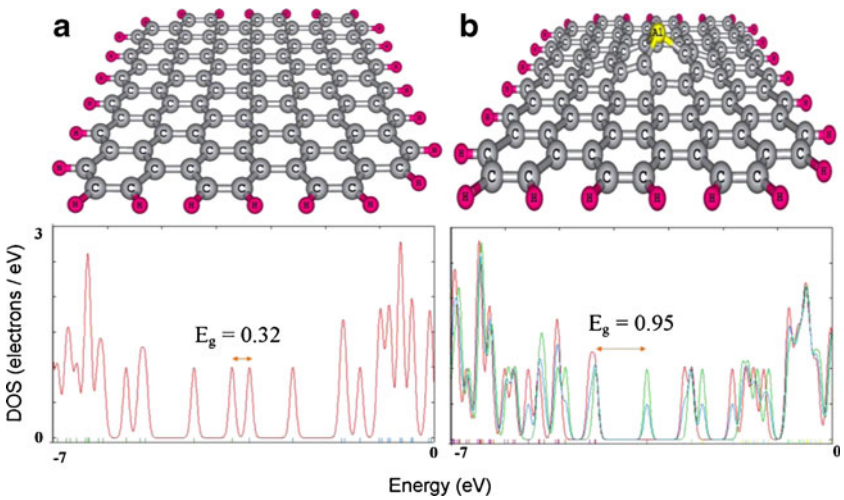

Fig. 1 Optimized structures of (a) pristine graphene and (b) Al-doped graphene and their density of states (DOS) plot. As Al-doped graphene is an open shell system (with an unpaired electron) in its DOS plots, the colors of red, green and blue designate spin up, spin down and total DOSs, respectively

Results and discussion

Adsorption of C_3H_4O on PG

The interaction of C_3H_4O with the PG was investigated by locating the molecule from its O, C or H atom on a C atom or on the center of a hexagonal ring. In most initial configurations the molecule was reoriented upon the optimization to a structure like configuration A in Fig. 2. Upon the geometric and energetic parameters which are summarized in Table 1, four stable states for C_3H_4O/PG complexes can be identified (A-D, Fig. 2).

As seen in Fig. 2a, a strong interaction occurred (E_a= −50.43 kcal mol^{-1}) with a separation of about 1.56 Å between the PG and C_3H_4O (configuration A) so that the planar surface of the PG is deformed and the C-O bond in C_3H_4O elongated from 1.21 to 1.44 Å. Also, three other stable configurations (with relatively similar E_a) are yielded (Table 1) in which the molecule is perpendicular to the PG surface. Mulliken charge analysis shows that about 0.01 |*e*| transfers from the PG to the C_3H_4O in all configurations except in A, in which, the molecule accepts about 0.13 |*e*| from the PG. This charge-transfer mechanism is illustrated in Fig. 3, which was generated by an electron density distribution

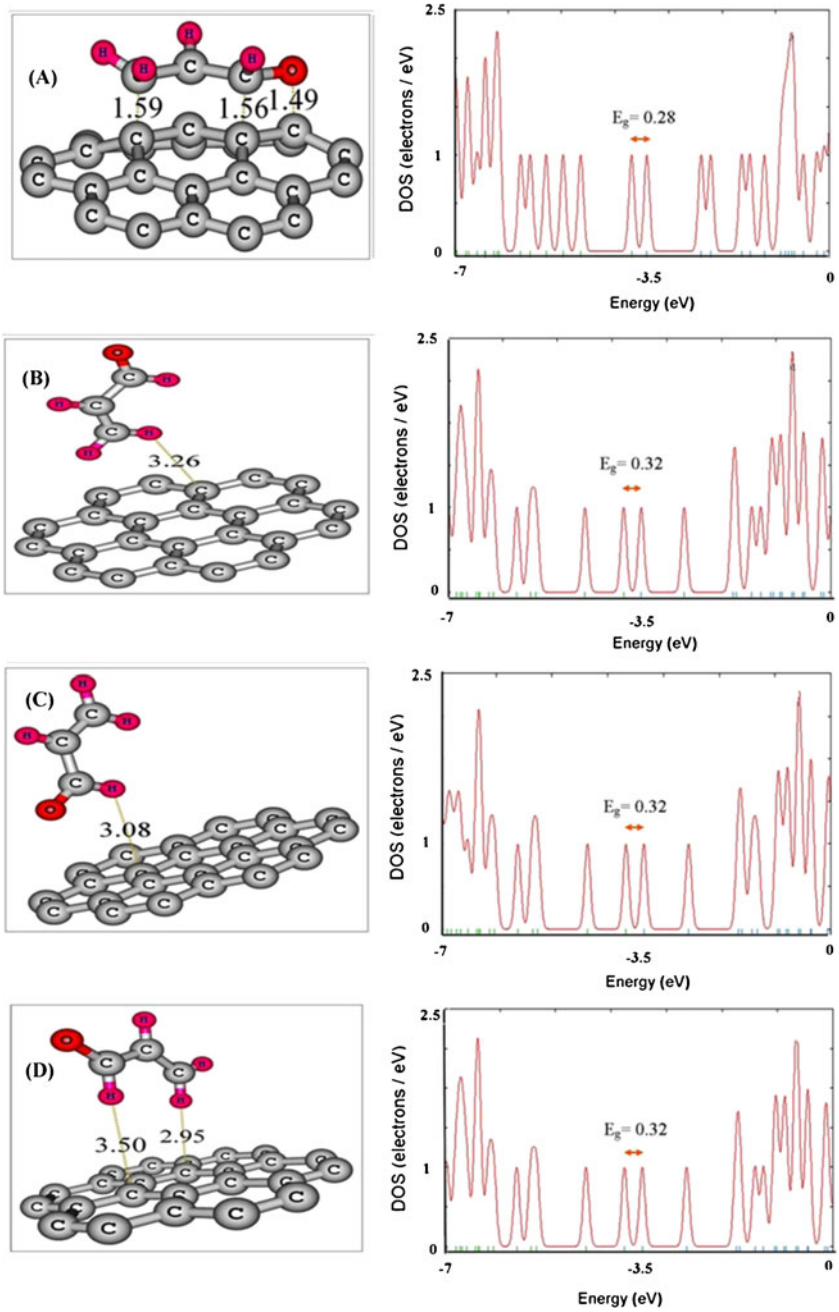

Fig. 2 Optimized structures for C_3H_4O/pristine-graphene complexes (Table 1) and their density of states (DOS) plots

Table 1 Calculated binding energy (E_a, kcal mol^{-1}), the nearest distance between the molecule and the PG surface (D), charge transfer from the SiG to the C_3H_4O (Q), HOMO energies (E_{HOMO}), LUMO energies (E_{LUMO}), energy of Fermi level (E_{FL}), HOMO/LUMO energy gap (E_g) in eV, and change in HOMO/LUMO gap (ΔE_g) of systems due to molecule adsorption

Systems	E_a	D (Å)	Q^* (e)	E_{HOMO}	E_{FL}	E_{LUMO}	E_g	% ΔE_g
PG	–	–	–	−3.71	−3.55	−3.39	0.32	–
A	−50.43	1.56	−0.13	−3.40	−3.54	−3.68	0.28	12.5
B	−1.15	3.26	−0.01	−3.46	−3.62	−3.78	0.32	0
C	−0.92	3.08	−0.01	−3.35	−3.51	−3.67	0.32	0
D	−0.92	2.95	−0.01	−3.43	−3.59	−3.75	0.32	0

* A negative number means charge transfer from PG to molecule

method using molecular electrostatic potential (MEP). Electrostatic potential surfaces can be displayed as an isocontour surface or mapped onto the molecular electron density. The blue regions show the most electron deficient region and the red color areas show the most electron accumulation regions. From the figure it can be found that there is a strong electron accumulation on C_3H_4O's oxygen atom whereas electron deficient areas are located on PG's carbon atoms near interaction sites. Due to the electronegativity differences between oxygen and carbon atoms, accumulation of electrons on the oxygen atom seems to be expectable. The significant interaction of toxic molecule with PG sheet here suggests a possible way for sensor applicability of PG for C_3H_4O detection. Motivated by such a possibility, we have explored changes in the electronic properties of PG with adsorbed molecule.

By comparing the DOS of PG with those of PG/C_3H_4O complexes, it can be seen that in the configuration A, the DOSs of PG are more altered upon C_3H_4O adsorption whereas no distinct changes are seen in others especially near the Fermi level (E_F, Table 1). Since occupied electronic levels with energy close to the E_F are proposed to be responsible for the optical and electronic properties of a material, it can be concluded that PG-based nanostructures cannot be suitable for the C_3H_4O detection. Additionally, the weak changes in E_g would probably not induce a large electric conductivity enhancement. On the other hand, the significant value of E_a points that the reproducibility of PG probably would be a time-consuming process and is not convenient for sensor designing. Considering all calculated parameters, it can be concluded that PG cannot be a good sensor material for C_3H_4O detection.

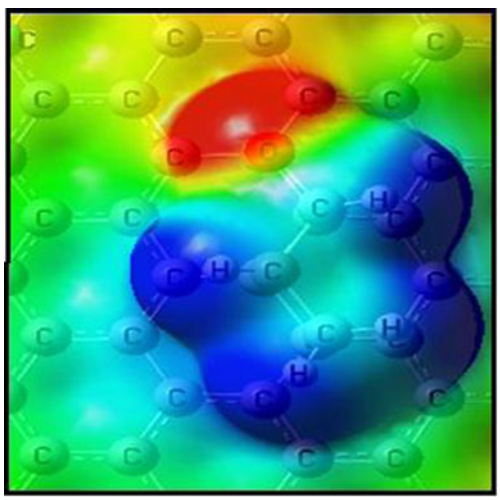

Fig. 3 The molecular electrostatic potential surface for adsorption of C_3H_4O on pristine graphene (configuration A in Fig. 2). The surfaces are defined by the 0.0004 electrons/b3 contour of the electronic density. Color ranges, in a.u.: blue, more positive than 0.010; green, between 0.010 and 0; yellow, between 0 and − 0.015; red, more negative than − 0.015

Adsorption of C_3H_4O on AlG

Due to the disadvantages of PG for C_3H_4O detection, we examined another chance for introducing a sensitive sensor for detection of C_3H_4O. Both theoretical and experimental studies have indicated that the chemical properties of carbon nanomaterials can be changed by doping with metal impurities. The sensing properties of AlG and SiG have been studied theoretically [18, 24, 25]. When one carbon atom in PG textile is replaced by one Al atom, the planar structure of PG surface undergoes drastic changes similar to the restructuring in Al-doped single wall carbon nanotubes [21]. As the Al atom is larger than carbon, it extrudes outward from the PG surface, resulting in some structural deformation which is more obvious near the doping site. The stable structure of AlG is shown in Fig. 1b. In order to investigate the interaction of C_3H_4O with AlG, the molecule was positioned above the Al atom of AlG sheet from its O, H and carbon atoms. After structural optimization, we found two complexes with negative E_a (E and F configuration in Fig. 4) which their detailed information including geometric parameters and the charge transfer values are summarized in Table 2. As seen in this Table, the E_a for adsorption of C_3H_4O on AlG was calculated to be about −20.55 and −30.92 kcal mol^{-1} for E and F configurations, respectively. In addition to the significant values of E_a, the

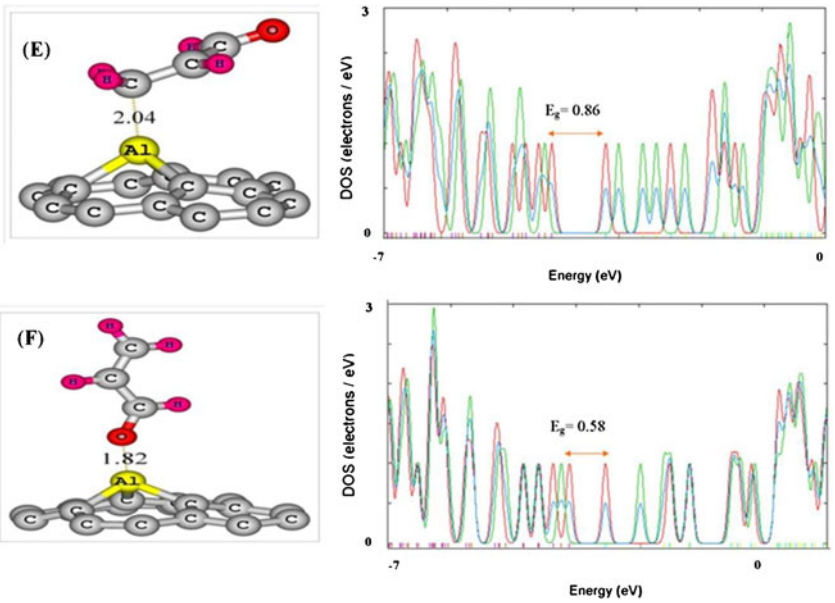

Fig. 4 Schematic views of the energetically favorable configurations of C_3H_4O/Al-doped graphene complexes and their density of states (DOS) plots

short molecule-sheet distance (1.82 Å, configuration F) indicates that when a C_3H_4O molecule is close to the surface of AlG, a strong interaction can be expected. The changes in the electron accumulation on the AlG after the adsorption of C_3H_4O, calculated by Mulliken charge analysis, illustrate that the greatest charge transfer between C_3H_4O and AlG (0.30 |e|) is obtained when the molecule aligned parallel to the AlG surface.

As it was shown before, two kinds of adsorption process can be found on the PG, namely; parallel (**A**, Fig. 2) and perpendicular (**B**, **C**, and **D**, Fig. 2) adsorptions. In the parallel adsorption the C_3H_4O molecule lies on the surface of the PG so that all its carbon and some hydrogen atoms participate in the interaction. While in the perpendicular adsorption almost one or two atoms of the molecule interacts with the surface of the PG. Figure 4 shows that the adsorption processes on the AlG are also perpendicular, but these processes are much stronger than the perpendicular adsorption on the PG. The charge analysis reveals that electrons tend to transfer from the sheets to the acrolein molecule (Tables 1 and 2). On the other hand, our frontier molecular analysis (FMO) indicates that the AlG has a singly occupied molecular orbital and its unpaired electron energetically has more tendency than the paired electrons of HOMO in the PG to shift to the LUMO of acrolein. Also, comparing the results of Tables 1 and 2 confirms that the charge transfer in the case of AlG is more than that in the PG. Our FMO analysis shows that the SOMO is mainly localized on the doped Al atom (Fig. 5), thereby causing to the stronger adsorption process in this case.

As shown in Fig. 1, in the AlG sublattice symmetry breaks and its E_g, is opened by about 0.63 eV, compared to the E_g of PG. Also, the structural parameters of AlG were compared to those of Sun et al. [4]. The comparison shows that our results are in good agreement with theirs. For further understanding adsorption characteristics of C_3H_4O on AlG, the DOSs for AlG/C_3H_4O complexes were calculated, and shown in Fig. 4. The DOS plots show that there is a considerable hybridizing between C_3H_4O and AlG orbitals which would lead to an electronic properties change of AlG upon adsorption of C_3H_4O molecule. Compared to the AlG, in the most stable configuration (E) new peaks appear at −4.11 (HOMO) and −5.53 (LUMO) eV, thereby closing the E_g of the AlG by about 0.37 eV. The changes in the DOS, especially in the region near the E_F, are expected to bring concerning changes in the corresponding electronic

Table 2 Calculated binding energy (E_a, kcal mol^{-1}), the nearest distance between the molecule and the AlG surface (D), charge transfer from the AlG to the C_3H_4O (Q), HOMO energies (E_{HOMO}), LUMO energies (E_{LUMO}), energy of Fermi level (E_{FL}), HOMO/LUMO energy gap (E_g) in eV, and change in E_g (ΔE_g) of systems due to molecule adsorption

Systems	E_a	D (Å)	Q * (e)	E_{HOMO}	E_{FL}	E_{LUMO}	E_g	$\%\Delta E_g$
AlG	–	–	–	−4.35	−3.88	−3.40	0.95	–
E	−20.55	2.04	−0.30	−4.34	−3.92	−3.48	0.86	9.0
F	−30.92	1.82	−0.18	−4.11	−3.82	−3.53	0.58	33

* A negative number means charge transfer from AlG to molecule

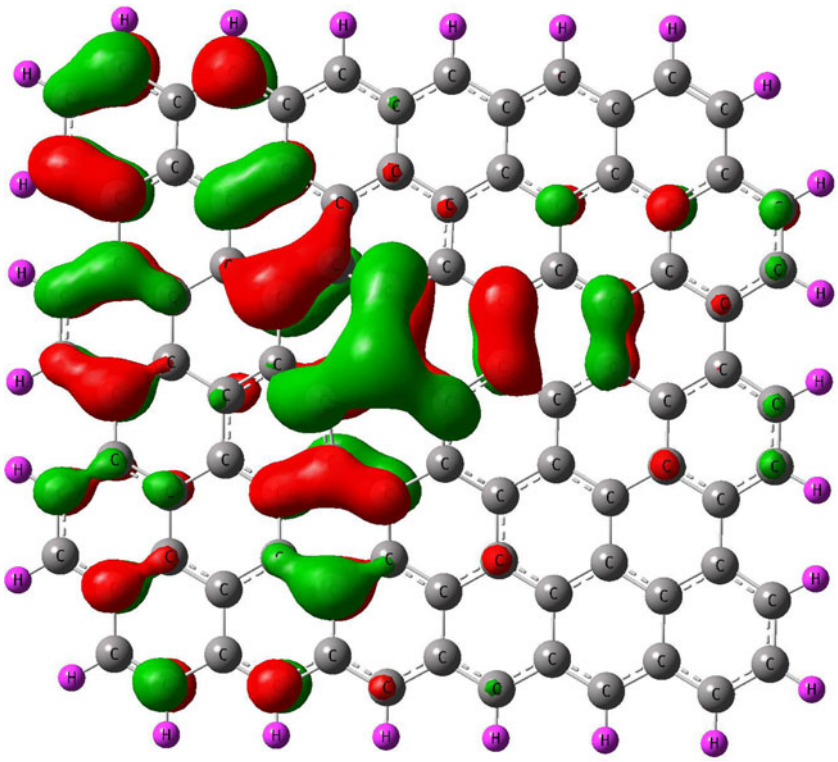

Fig. 5 The profile of singly occupied molecular orbital which is mainly located on the Al atom of the Al-doped graphene sheet

properties, which is beneficial for sensing applications. Upon the following equation [26]:

$$\sigma \propto \exp\left(\frac{-E_g}{2kT}\right). \quad (2)$$

It is found that in a fixed temperature, decrease in E_g energy increases electric conductivity of conducting material (where σ is electric conductivity and k is the Boltzmann's constant). Table 2 indicates that the E_g experiences changes about 9.0 % (from 0.95 to 0.85 eV) and 33 % (from 0.95 to 0.58 eV) in E and F configurations, respectively. The change in the value of E_g in the F configuration is significant, so as said before, considerable changes in the corresponding electronic properties of AlG are expected. Consequently, it can be expected that through the following changes in the AlG's conductivity before and after the adsorption process, the presence of C_3H_4O could be detected sensitively.

Table 3 Structure parameters of the favorite adsorption configuration (F configuration) and charge transfer (Q) between the AlG and the C_3H_4O molecule under different field intensity (F^*)

	F=−0.03	F=−0.02	F=−0.01	F=0.00	F=0.01
O-Al	1.76	1.80	1.86	1.82	1.96
C-Al	1.95	1.91	1.87	1.84	1.90
Q**	0.54	0.44	0.33	−0.18	−0.54

* The field intensity is a. u

** The charge transfer is obtained by Mulliken analysis. The reported C-Al is average binding length of three C-Al in AlG in Å

The effect of an external electric field on the adsorption/desorption behaviors of AlG/ C_3H_4O complex

A promising gas sensor, in addition its high sensitivity and good selectivity, should have another important factor: reproducibility. There are several reported methods for reactivation of graphene sensor materials. The important fact is that graphene sensing properties are fully recoverable either by thermal annealing [12] or by the UV illumination for short time [27, 28]. Ko et al. exposed their developed graphene-based NO_2 detector to a repeated cycling of ambient gases from air to NO_2. In their experiment, there was no sign of deterioration in the sensitivity of graphene-based gas sensor [29]. Also it has been reported that sensors can be used for alternative applications by applying an external electric field

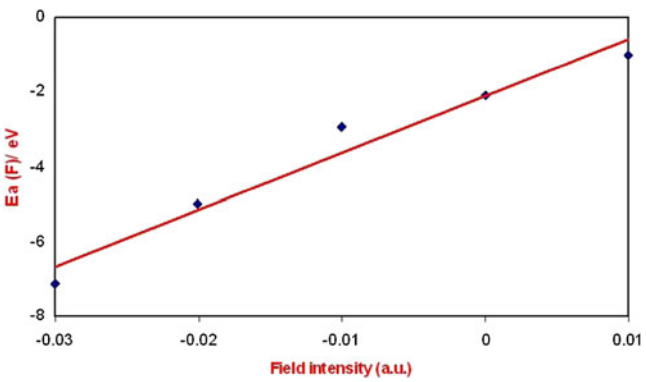

Fig. 6 E_a of C_3H_4O molecule adsorbed on AlG (configuration E) vs. intensity of the used electric field. The line is the fitted R^2 line

[30]. The quantum mechanical calculations for influence of electric field on adsorption/desorption behavior of particles on an absorbent surfaces was firstly carried out by Tomanek et al. [31]. They applied electric field for N_2 molecules which were adsorbed on Fe (111) surface. The CO molecules on AlG are reported to be desorbed by applying an external electric field of 0.03 a.u. due to the large upward force on CO molecule induced by electrical field [32]. Due to large amount of E_a in the adsorption of C_3H_4O on the AlG surface, it may be doubted, however, that the reproducibility of AlG should be almost impossible. Therefore, the reproducibility of AlG was one of the important parts in our study. The calculations here were limited to the most favorable configuration of C_3H_4O/AlG complex (F configuration). The field intensity was changed in the range of – 0.03 to 0.01 a.u. (1a.u.=5.14×10^{11}V/m). The negative values mean that the direction of field is reversed relative to its initial direction. In the absence of an external electric field, the electrons transfer from AlG to C_3H_4O is calculated to be about 0.18 |e|. It is expected that the charge transfer is affected by applying an electric field vertical to AlG surface (in the Z-axis direction). In these calculation steps, all the atoms were allowed to relax. A charged particle experiences a force when placed in a region where there exists an electric field. From the definition of the electric field, this force is given by Eq. 3:

$$\vec{F} = q\vec{E}. \tag{3}$$

Where $\vec{F}$ is the force exerted on the charged particle, q is the charge of the particle and $\vec{E}$ is the electric field. When an electron (q=−e) is in an electric field, the electron experiences a force in the direction opposite of the electric field. In the presence of different field intensities, the changes in the net charge transfer and bond lengths are scanned. Results summarized in Table 3 show that the changes in charge transfers values are relatively considerable, they also clarify that the C-Al bond length in AlG elongates while the O-Al bond length reduces as field intensity increases. Table 3 also reveals weakness of the O-Al bond occurs under the positive values of field despite its strength in the negative values. In addition to increase in bond lengths, significant structural deformation of AlG was also observed and the C-Al bond lengths elongates to the new ones. As electric field increases, deformations become more and more obvious, indicating that the C_3H_4O adsorption is affected significantly by external electric field. To approximate the effects of an electric field on the adsorption process, we estimated the E_a under electric field (E_a (F)) which is defined as follows:

$$E_a(F) = E_{C_3H_4O+AlG}(F) - [E_{AlG}(F) + E_{C_3H_4O}(F)], \tag{4}$$

where the subscripts C_3H_4O +AlG, AlG and C_3H_4O indicate the adsorbed system, the initial isolated AlG surface and the C_3H_4O molecule totally under electric field, respectively. The corresponding results after adsorption which are plotted in Fig. 6 indicate that the E_a (F) increases nearly linearly as field increases. From the decrease in O-Al distance in addition to increase in E_a (F), it can be concluded that adsorption of C_3H_4O on the AlG can be significantly strengthened by using negative external electric field. The approximate linear relationship between E_a (F) and field intensity can be explained by the first-order Stark effect. The largest value of the Al-O bond length (1.96 Å) was obtained in the electric field strength of 0.01 a.u, indicating more weakening of this bond. All these observations indicate that if the field intensity increases to high values, desorption of C_3H_4O might occur probably. Thus, it can be expected that the highly positive electric field can be used to reactivate the AlG sensor material for repetitive applications. It has been previously shown [33, 34] that the intermolecular hydrogen bond is significantly strengthened upon photoexcitation to the excited state compared with that in the ground state. It seems that, the external electronic field may act similar to the light and affects the intermolecular interaction by shifting the molecular orbitals.

Conclusions

To summarize, quantum chemical calculation by DFT using X3LYP method is performed to investigate adsorption sensitivity of both PG and AlG in the presence of C_3H_4O. The calculated geometric and energetic parameters such as net electron transfer, MEP plot and the DOS spectrums suggest that the adsorption of C_3H_4O on PG is almost by strong adsorption in nature whereas on AlG is by somewhat weak adsorption. The net charge transfer values are found to be larger for AlG rather than those for PG system. Furthermore, the DOS plots show that overlap of C_3H_4O orbitals with AlG leads to a large decrease in E_g of AlG. Compared to PG, AlG has a higher sensitivity toward the C_3H_4O molecules. The strong interactions between AlG and the adsorbed molecules induce dramatic changes to the electronic properties of AlG and make it a promising candidate as a gas sensing material for detection of C_3H_4O. AlG containing adsorbed C_3H_4O molecules might be reactivated by applying an external electric field if electric field intensity increases more than 0.1 a.u.

References

1. Martínez I, Ordóñez A, Guerrero J, Pedersen S, Miñano A, Teruel R, Velázquez L, Kristensen SR, Vicente V, Corral J (2009) Effects of acrolein, a natural occurring aldehyde, on the anticoagulant serpin antithrombin. FEBS Lett 583(19):3165–3170
2. Roy J, Pallepati P, Bettaieb A, Tanel A, Averill-Bates DA (2009) Acrolein induces a cellular stress response and triggers mitochondrial apoptosis in A549 cells. Chem Biol Interact 181(2):154–167

3. Sithu SD, Srivastava S, Siddiqui MA, Vladykovskaya E, Riggs DW, Conklin DJ, Haberzettl P, O'Toole TE, Bhatnagar A, D'Souza SE (2010) Exposure to acrolein by inhalation causes platelet activation. Toxicol Appl Pharmacol 248(2):100–110
4. Sun Y, Chen L, Zhang F, Li D, Pan H, Ye J (2010) First-principles studies of HF molecule adsorption on intrinsic graphene and Al-doped graphene. Solid State Commun 150(39):1906–1910
5. Christofides C, Mandelis A (1990) Solid–state sensors for trace hydrogen gas detection. J Appl Phys 68(6):R1–R30
6. Chen Z, Lin YM, Rooks MJ, Avouris P (2007) Graphene nano-ribbon electronics. Physica E 40(2):228–232
7. Dragoman M, Dragoman D (2009) Graphene-based quantum electronics. Prog Quant Electron 33(6):165–214
8. Hass J, De Heer W, Conrad E (2008) The growth and morphology of epitaxial multilayer graphene. J Phys Condens Matter 20(32):323202
9. Myers M, Cooper J, Pejcic B, Baker M, Raguse B, Wieczorek L (2011) Functionalized graphene as an aqueous phase chemiresistor sensing material. Sens Actuat-B 155(1):154–158
10. Novoselov K, Geim A, Morozov S, Jiang D, Zhang Y, Dubonos S, Grigorieva I, Firsov A (2004) Electric field effect in atomically thin carbon films. Science 306(5696):666–669
11. Kuila T, Bose S, Khanra P, Mishra AK, Kim NH, Lee JH (2011) Recent advances in graphene-based biosensors. Biosens Bioelectron 26(12):4637–4648
12. Schedin F, Geim A, Morozov S, Hill E, Blake P, Katsnelson M, Novoselov K (2007) Detection of individual gas molecules adsorbed on graphene. Nat Mater 6(9):652–655
13. Huang B, Li Z, Liu Z, Zhou G, Hao S, Wu J, Gu BL, Duan W (2008) Adsorption of gas molecules on graphene nanoribbons and its implication for nanoscale molecule sensor. J Phys Chem C 112(35):13442–13446
14. Leenaerts O, Partoens B, Peeters FM (2008) Adsorption of H2 O, N H3, CO, N O2, and NO on graphene: A first-principles study. Phys Rev B Condens Matter Mater Phys 77(12)
15. Fowler JD, Allen MJ, Tung VC, Yang Y, Kaner RB, Weiller BH (2009) Practical chemical sensors from chemically derived graphene. ACS Nano 3(2):301–306
16. Romero HE, Joshi P, Gupta AK, Gutierrez HR, Cole MW, Tadigadapa SA, Eklund PC (2009) Adsorption of ammonia on graphene. Nanotechnology 20(24):245501
17. Rastegar SF, Peyghan AA, Hadipour NL (2013) Response of Si-and Al-doped graphenes toward HCN: A computational study. Appl Surf Sci 265:412–417
18. Qin X, Meng Q, Zhao W (2011) Effects of Stone–Wales defect upon adsorption of formaldehyde on graphene sheet with or without Al dopant: a first principle study. Surf Sci 605(9):930–933
19. Schmidt MW, Baldridge KK, Boatz JA, Elbert ST, Gordon MS, Jensen JH, Koseki S, Matsunaga N, Nguyen KA, Su S (2004) General atomic and molecular electronic structure system. J Comput Chem 14(11):1347–1363
20. Xu X, Goddard WA (2004) The X3LYP extended density functional for accurate descriptions of nonbond interactions, spin states, and thermochemical properties. Proc Natl Acad Sci U S A 101(9): 2673–2677
21. Ao Z, Yang J, Li S, Jiang Q (2008) Enhancement of CO detection in Al doped graphene. Chem Phys Lett 461(4):276–279
22. Tachikawa H, Nagoya Y, Fukuzumi T (2010) J Power Sources 195(18):6148–6152
23. Shemella P, Zhang Y, Mailman M, Ajayan PM, Nayak SK (2007) Appl Phys Lett 91(4):042101–042103
24. Zou Y, Li F, Zhu Z, Zhao M, Xu X, Su X (2011) An ab initio study on gas sensing properties of graphene and Si-doped graphene. Euro. Phys J B 81:475–479
25. Wang R, Zhang D, Sun W, Han Z, Liu C (2007) A novel aluminum-doped carbon nanotubes sensor for carbon monoxide. J Mol Struct (THEOCHEM) 806:93–97
26. Li SS (1993) Semiconductor physical electronics. Plenum, New York
27. Shi Y, Fang W, Zhang K, Zhang W, Li LJ (2009) Photoelectrical Response in Single–Layer Graphene Transistors. Small 5:2005–2011
28. Lin J, Zhong J, Kyle JR, Penchev M, Ozkan M, Ozkan CS (2011) Molecular absorption and photodesorption in pristine and functionalized large-area graphene layers. Nanotechnology 22(35):355701
29. Ko G, Kim HY, Ahn J, Park YM, Lee KY, Kim J (2010) Graphene-based nitrogen dioxide gas sensors. Curr Appl Phys 10(4):1002–1004
30. Hyman MP, Medlin JW (2005) Theoretical study of the adsorption and dissociation of oxygen on Pt (111) in the presence of homogeneous electric fields. J Phys Chem B 109(13):6304–6310
31. Tománek D, Kreuzer HJ, Block JH (1985) Tight-binding approach to field desorption: N 2 ON Fe(111). Surf Sci 157(1):L315–L322
32. Acharya CK, Turner C (2007) Effect of an electric field on the adsorption of metal clusters on boron-doped carbon surfaces. J Phys Chem C 111(40):14804–14812
33. Zhao G-J, Han K-L (2011) Hydrogen bonding in the electronic excited state. Acc Chem Res 45(3):404–413
34. Zhao GJ, Han KL (2008) Effects of hydrogen bonding on tuning photochemistry: concerted hydrogen–bond strengthening and weakening. Chemphyschem 9(13):1842–1846